Bioorganic & Medicinal Chemistry 24 (2016) 2707–2715

Contents lists available at ScienceDirect

Bioorganic & Medicinal Chemistry

journal homepage: www.elsevier.com/locate/bmc

Design, synthesis, and biological evaluation of substrate-competitive inhibitors of C-terminal Binding Protein (CtBP)

Sudha Korwar [a,†], Benjamin L. Morris [b,†], Hardik I. Parikh [a], Robert A. Coover [a], Tyler W. Doughty [c], Ian M. Love [b], Brendan J. Hilbert [d], William E. Royer, Jr. [d], Glen E. Kellogg [a], Steven R. Grossman [b,*], Keith C. Ellis [a,*]

[a] Department of Medicinal Chemistry, School of Pharmacy, The Institute for Structural Biology, Drug Discovery, and Development, and the Massey Cancer Center, Virginia Commonwealth University, Richmond, VA 23298, United States
[b] Division of Hematology, Oncology, & Palliative Care, Department of Human and Molecular Genetics, and the Massey Cancer Center, Virginia Commonwealth University, Richmond, VA 23298, United States
[c] Department of Molecular, Cell, & Cancer Biology, University of Massachusetts Medical School, Worcester, MA 01605, United States
[d] Department of Biochemistry & Molecular Pharmacology, University of Massachusetts Medical School, Worcester, MA 01605, United States

ARTICLE INFO

Article history:
Received 1 March 2016
Revised 14 April 2016
Accepted 19 April 2016
Available online 20 April 2016

Keywords:
C-terminal Binding Protein
CtBP
MTOB
Hydroxyimine
Oxime
Transcriptional co-repressor
Dehydrogenase
Tumor suppressor gene

ABSTRACT

C-terminal Binding Protein (CtBP) is a transcriptional co-regulator that downregulates the expression of many tumor-suppressor genes. Utilizing a crystal structure of CtBP with its substrate 4-methylthio-2-oxobutyric acid (MTOB) and NAD^+ as a guide, we have designed, synthesized, and tested a series of small molecule inhibitors of CtBP. From our first round of compounds, we identified 2-(hydroxyimino)-3-phenylpropanoic acid as a potent CtBP inhibitor (IC_{50} = 0.24 μM). A structure–activity relationship study of this compound further identified the 4-chloro- (IC_{50} = 0.18 μM) and 3-chloro- (IC_{50} = 0.17 μM) analogues as additional potent CtBP inhibitors. Evaluation of the hydroxyimine analogues in a short-term cell growth/viability assay showed that the 4-chloro- and 3-chloro-analogues are 2-fold and 4-fold more potent, respectively, than the MTOB control. A functional cellular assay using a CtBP-specific transcriptional readout revealed that the 4-chloro- and 3-chloro-hydroxyimine analogues were able to block CtBP transcriptional repression activity. This data suggests that substrate-competitive inhibition of CtBP dehydrogenase activity is a potential mechanism to reactivate tumor-suppressor gene expression as a therapeutic strategy for cancer.

1. Introduction

C-terminal Binding Protein (CtBP) is a transcriptional co-regulator known to repress tumor suppressor genes and activate proto-oncogenes, and is overexpressed in a majority of colon,[1] breast,[2] and ovarian[3] cancers. The endogenous function of CtBP is to regulate gene expression by interacting with DNA-binding transcription factors and to recruit repressor or activator complexes to targeted promoters. These transcription complexes, which include histone deacetylases,[4] histone methyltransferases,[5] and other chromatin-modifying proteins,[6] modify the target gene epigenetically to silence or activate its expression.

Multiple tumor suppressor genes are repressed by CtBP including *E-cadherin*,[7] *PTEN*,[8] the apoptosis genes *Bik*, *Noxa*, *Puma*, and *PERP*,[9] and the breast cancer susceptibility gene *Brca1*.[2] Repression of these tumor suppressor genes by CtBP promotes multiple pro-oncogenic activities, including epithelial-mesenchymal transition (EMT),[7] cell migration and invasion,[8,10,11] and cell survival.[7,12] Oncogenes and cancer relevant genes activated by CtBP include *TIAM1* and the *MDR1* gene, which promote metastasis and chemotherapeutic drug efflux and resistance, respectively.[13] Genomic studies[14] have shown that: (1) CtBP expression induces mesenchymal and stem cell-like features, (2) multiple CtBP repression gene targets are selectively downregulated in aggressive breast cancer subtypes, (3) differential expression of CtBP-targeted genes predicts poor clinical outcome in breast cancer patients, and (4) elevated levels of CtBP in patient tumors predict shorter median survival.

CtBP is activated as a transcriptional co-regulator under conditions of hypoxia or glycolysis where NADH levels are

* Corresponding authors.
E-mail addresses: kcellis@vcu.edu (K.C. Ellis), steven.grossman@vcuhealth.org (S.R. Grossman).
† These authors contributed equally to this work.

http://dx.doi.org/10.1016/j.bmc.2016.04.037
0968-0896/

elevated,[15] as might be found in hypoxic tumors or those undergoing aerobic glycolysis (the Warburg effect). Under conditions with a low concentration of NADH, CtBP remains in an inactive, monomeric form. Elevation of NADH levels results in dimerization of two CtBP subunits into the transcriptionally active form of the protein.[16–19] In this manner, CtBP acts as an intracellular metabolic sensor of NADH concentration.

Inhibition of CtBP's transcriptional co-regulatory activity has been shown to reverse the neoplastic phenotype. Depletion of CtBP using siRNA restored expression of mRNA from repressed target genes, synthesis of the gene product by translation, and protein function.[2] A cyclic peptide (cyclo-SGWTVVRMY) has been reported that inhibits CtBP dimerization in vitro and in cells by binding to an allosteric site.[20] This peptide reduced mitotic fidelity, proliferation, and colony forming potential in cancer cells. A small molecule that disrupts CtBP association with a transcriptional partner has also been reported.[21]

In addition to acting as a transcriptional co-regulator, CtBP contains a catalytically active dehydrogenase domain that binds both NADH and a putative substrate, 4-methylthio-2-oxobutyric acid (MTOB, **1**, Fig. 1a).[22] The dehydrogenase active site catalyzes the reduction of the ketone in MTOB (**1**) to the alcohol in the product 4-methylthio-2-hydroxy-butyric acid (MTHB, **2**), converting NADH to NAD^+ in the process (Fig. 1a).

Pharmacological inhibition of CtBP's dehydrogenase activity also reverses the cancer phenotype and induces apoptosis. High concentrations of MTOB substrate (**1**) inhibits the dehydrogenase activity of recombinant CtBP in vitro (IC_{50} = 300 μM), disrupts transcriptional repression/activation, promotes the expression of the BH3 protein Bik in $p53^{-/-}$ HCT-116 colon cells, and is specifically cytotoxic to both wild-type and $p53^{-/-}$ HCT-116 cells but not MEF cells.[1] Further studies have shown that MTOB (**1**) disrupts transcriptional repression in breast cancer cell lines[14] and suppressed cell survival in an ovarian cell line with CtBP overexpression.[23]

Here we report the design, synthesis, and biological evaluation of small molecule inhibitors of CtBP's dehydrogenase activity. From our first round of compounds, we identified 2-(hydroxyimino)-3-phenylpropanoic acid (**9**) as a potent CtBP inhibitor (IC_{50} = 0.24 μM). A structure–activity relationship study of this compound further identified the 4-chloro- and 3-chloro-analogues as additional potent CtBP inhibitors which not only inhibit the dehydrogenase activity in vitro but also restore the transcription of Bik, a CtBP target gene, in cells.

2. Results and discussion

2.1. First-generation substrate-competitive CtBP inhibitors

The crystal structure of MTOB (**1**) in complex with CtBP and NAD^+ has been reported (Fig. 1b).[24] The α-ketoacid functional group in MTOB (**1**) shows clear interactions with the CtBP catalytic triad (Arg97, Arg266, and His315). The sulfur atom in MTOB (**1**) is positioned ~4 Å from Trp318 and forms a sulfur–π-interaction with the indole ring.

Using the CtBP1/MTOB (**1**)/NAD^+ crystal structure as a starting point, we designed, synthesized, and evaluated small molecules that would inhibit the dehydrogenase activity of CtBP. Starting from MTOB (**1**, IC_{50} = 300 μM), the first modification was to replace the thioether with a phenyl ring in order to improve the π-interactions with Trp318 of CtBP (Scheme 1).

Phenylpyruvic acid (**3**) was tested for its ability to inhibit the reduction of MTOB (**1**) to MTHB (**2**) by CtBP in an NADH consumption assay. Phenylpyruvic acid (**3**) was found to be a ~3-fold better inhibitor than MTOB with an IC_{50} of 116 μM (see Table S1 in the Supplementary material).

While phenylpyruvic acid (**3**) does inhibit the dehydrogenase activity of CtBP, it also acts as a substrate for the enzyme. To stop this chemical reduction of phenylpyruvic acid (**3**) and improve inhibition of CtBP, we next designed compounds based on the phenylpyruvic acid structure that contained isosteres of the α-ketone that could not be reduced by NADH (Scheme 1). These compounds included α-thioketone **4**, acrylic acid **5**, malonic acid **6**, amide **7**, hydrazone **8**, and hydroxyimine **9**. All of these compounds were either synthesized or purchased and tested for their ability to inhibit CtBP. While most of these compounds were less active than

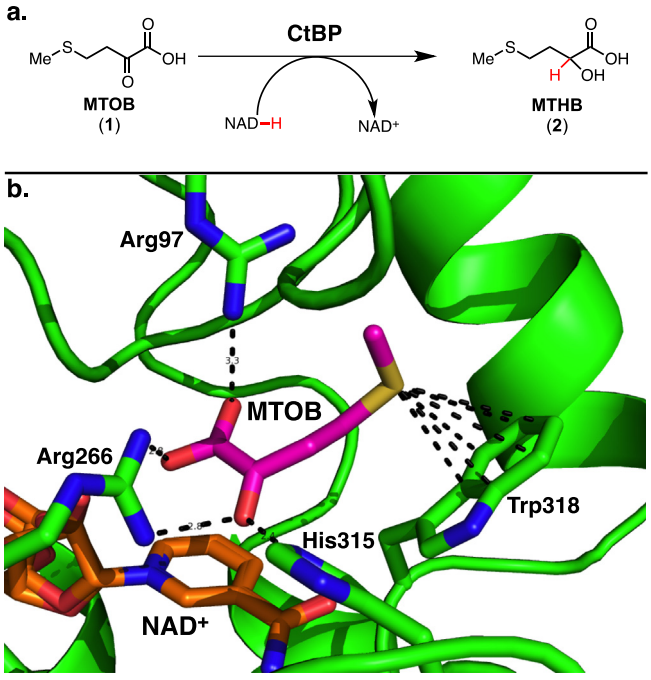

Figure 1. (a) Enzymatic reaction catalyzed by CtBP. (b) Crystal structure of CtBP1 with MTOB (**1**) and NAD^+ (PBDID: 4LCE).

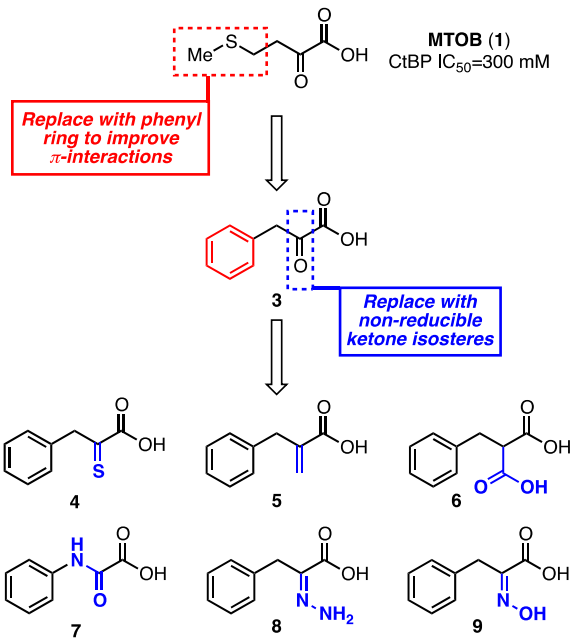

Scheme 1. Design of CtBP Inhibitors from MTOB (**1**).

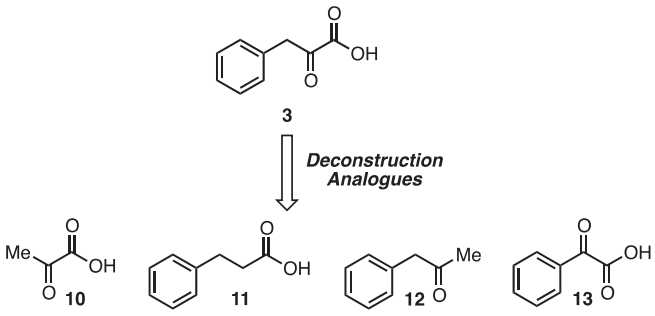

Scheme 2. Design of deconstruction analogues of phenylpyruvic acid (**3**).

phenylpyruvic acid itself (Table S1), hydroxyimine **9** inhibited CtBP with an IC_{50} of 0.24 μM, a ~480-fold improvement. Hydroxyimine **9** was therefore chosen for further structure–activity relationship studies. In these studies, none of the compounds with a bioisosteric replacement for the α-ketone (**4**–**9**) acted as a substrate for CtBP.

In parallel with the ketone isosteres, we also prepared a series of deconstruction analogues of **3** to determine which structural features were necessary for inhibition (Scheme 2). These deconstruction analogues included: pyruvate **10**, where the phenyl ring has been removed; hydrocinnamic acid **11**, where the ketone has been removed; 1-phenylpropan-2-one **12**, where the carboxylic acid has been removed; and phenylglyoxylic acid **13**, where the methylene spacer between the phenyl ring and the α-ketoacid has been removed. These compounds were also either synthesized or purchased and tested for their ability to inhibit CtBP. All of these compounds were less active than phenylpyruvic acid (Table S1).

2.2. Structure–activity relationship studies on the hydroxyimine scaffold

With an understanding of the minimum structural elements needed to inhibit CtBP, we designed a large set of analogues based on the best inhibitor from our first set of compounds, hydroxyimine **9**. For this set, we chose to focus on exploring the structure–activity relationship of the phenyl ring. Our set of analogues included electronically and sterically diverse substituents; all were evaluated computationally by docking them into the site identified in the CtBP–**9** crystal structure[25] to prioritize synthesis and evaluation. Docking scores calculated with the HINT scoring function[26] (Table 1), which has been shown to correlate with free energy of binding, identified thirteen compounds that we selected for synthesis and evaluation as inhibitors of CtBP (**14a**–**m**, Fig. 2).

To synthesize the hydroxyimine analogues, we chose hydantoin chemistry as a general route that would offer the flexibility needed to introduce a variety of substituents on the phenyl ring (Scheme 3). Condensation of substituted benzaldehydes (**15a**–**b**, **d**–**g**, **i**–**m**) with hydantoin under basic conditions afforded the 5-benzylideneimidazolidine-2,4-diones (**16a**–**b**, **d**–**g**, **i**–**m**), which were then hydrolyzed to afford a variety of substituted phenylpyruvic acid analogues, which upon characterization were shown to exist as the enol tautomers (**17a**–**b**, **d**–**g**, **i**–**m**), as shown in Scheme 3. These phenylpyruvic acid analogues were then condensed with hydroxylamine to form the hydroxyimine analogues (**14a**–**b**, **d**–**g**, **i**–**m**). We found this synthetic route to be highly tolerant of substitutions on the starting benzaldehyde and were able to synthesize eleven of the thirteen analogues using this methodology. For the two compounds (**14c** and **14h**) where condensation

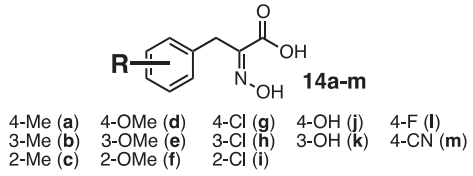

Figure 2. Analogues of **9** designed to explore the structure–activity relationship.

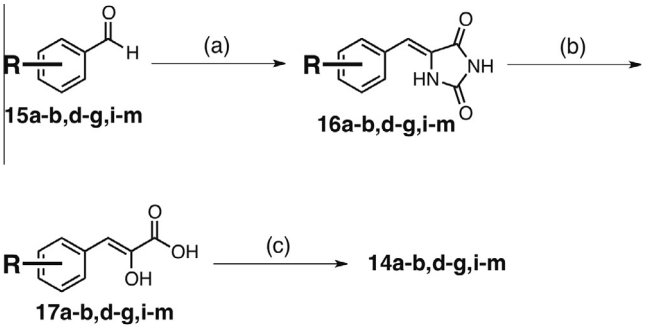

Scheme 3. Synthesis of analogues **14a**–**b**, **d**–**g**, and **i**–**m**. Reagents and conditions: (a) hydantoin, Na_2CO_3 (sat aq), ethanolamine, EtOH/H_2O (1:1), 120 °C, 5–10 h. (b) (i) 20% NaOH (aq), 100 °C, 3 h; 12 N HCl, 54–88% for 2 steps. (c) $NH_2OH{\cdot}HCl$, NaOH, H_2O, rt, 12 h, 54–91%.

Table 1
Inhibition of recombinant CtBP and Inhibition of cell growth of HCT-116 $p53^{-/-}$ colon cancer cells by cell growth/viability assay for hydroxyimine analogues

Compound	Substituent	HINT score	CtBP IC_{50}[a] (μM)	Cellular IC_{50}[a] (mM)	*C* Log *P*
9	H	963	0.24 (0.21, 0.27)	4.12 (2.96, 5.73)	1.36
14a	4-Me	946	0.32 (0.29, 0.37)	3.28 (2.51, 4.28)	1.86
14b	3-Me	756	0.48 (0.43, 0.54)	3.26 (2.71, 3.93)	1.86
14c	2-Me	1078	8.73 (6.19, 12.29	0.23 (0.16, 0.35)	1.81
14d	4-OMe	925	2.16 (1.19, 3.90)	1.93 (1.65, 2.25)	1.28
14e	3-OMe	919	0.88 (0.81, 0.97)	5.60 (3.56, 8.84)	1.28
14f	2-OMe	858	>100	1.24 (1.02, 1.51)	1.28
14g	4-Cl	861	0.18 (0.16, 0.20)	1.74 (1.47, 2.06)	2.07
14h	3-Cl	844	0.17 (0.15, 0.19)	0.85 (0.76, 0.96)	2.07
14i	2-Cl	974	7.65 (5.93, 9.86)	2.37 (1.83, 3.08)	2.07
14j	4-OH	767	7.34 (5.26, 10.25)	>10	0.69
14k	3-OH	1003	0.72 (0.67, 0.78)	>10	0.69
14l	4-F	n.d.[b]	0.30 (0.27, 0.33)	3.97 (3.52, 4.49)	1.50
14m	4-CN	574	0.90 (0.82, 0.98)	1.10 (0.81, 1.49)	0.79
MTOB (**1**)	—	n.d.[b]	n.d.[b]	4.0[c]	−0.34

[a] Data represents the averages with 95% confidence intervals shown in parentheses of three independent experiments.
[b] n.d. = not determined.
[c] From Ref. 1.

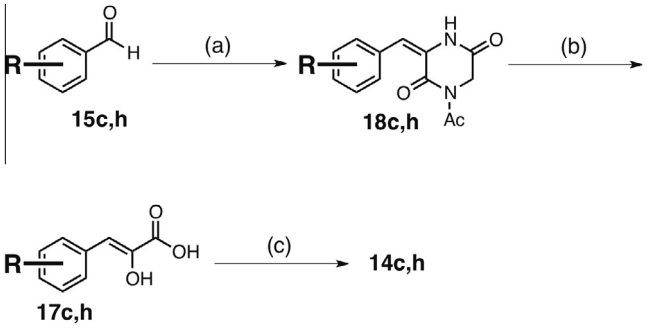

Scheme 4. Synthesis of analogues **14c** and **14h**. Reagents and conditions: (a) 1,4-diacetylpiperazine-2,5-dione, NEt_3, DMF, rt, 12 h. (b) 6 N HCl, reflux, 4 h; 58% (**17c**), 56% (**17h**). (c) $NH_2OH{\cdot}HCl$, NaOH, H_2O, rt, 12 h; 92% (**17c**), 66% (**17h**).

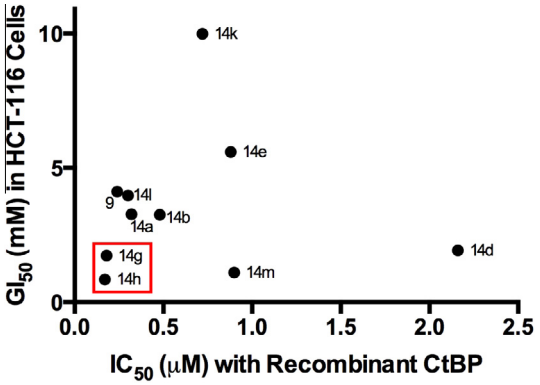

Figure 3. Plot of IC_{50} with recombinant enzyme (from NADH assay) versus GI_{50} from cell growth/viability assay for hydroxyimine analogues. The most potent compounds (**14g** and **14h**) are highlighted by the red box. Analogues **14c**, **14f**, **14i**, and **14j** have been omitted for clarity.

of the benzaldehyde with the hydantoin failed to afford the 5-benzylideneimidazolidine-2,4-dione, we used the alternative methodology shown in Scheme 4. This alternative method utilized a condensation of benzaldehydes **15c** and **15h** with 1,4-diacetylpiperazine-2,5-dione to afford the 1-acetyl-3-benzylidenepiperazine-2,5-diones **18c** and **18h**. These intermediates were then hydrolyzed to afford the phenylpyruvic acid analogues **17c** and **17h**, which were also found to exist as the enol tautomers, followed by condensation with hydroxylamine to form the hydroxyimine analogues **14c** and **14h**.

Hydroxyimine analogues **14a–m** were tested for their ability to inhibit the functional dehydrogenase activity of CtBP in an NADH consumption assay. Relative to the parent hydroxyimine **9**, we observed that ortho-substitutions on the ring were detrimental to inhibitory activity [**14c** (2-Me), **14f** (2-OMe), **14i** (2-Cl), Table 1]. *para*- and *meta*-substitution by electron-donating groups [**14d** (4-OMe), **14e** (3-OMe), **14j** (4-OH),**14k** (3-OH)] resulted in a large decrease in inhibitory activity, while *para*- and *meta*-substitution by the electronically neutral methyl group [**14a** (4-Me), **14b** (3-Me)] resulted in only a small decrease in inhibitory activity. However, *para*- and *meta*-substitution by an electron-withdrawing chlorine group [**14g** (4-Cl), **14h** (3-Cl)] resulted in analogues that were more active as inhibitors than parent hydroxyimine **9**. Interestingly, this effect seems specific to chlorine, as *para*-substitutions with other electron-withdrawing groups [**14l** (4-F), **14m** (4-CN)] resulted in no increase in inhibition (**14l**) or a decrease in inhibitory activity (**14m**). The three best inhibitors, hydroxyimines **9**, **14g**, and **14h**, were tested for off-target inhibition of lactate dehydrogenase (LDH), a metabolic dehydrogenase with a catalytic mechanism similar to CtBP. All three hydroxyimines were >170-fold selective for CtBP2 over LDH [**9**: LDH IC_{50} = 42.5 ± 1.1 μM; **14g**: LDH IC_{50} = 181.9 ± 12.9 μM; and **14h**: LDH IC_{50} = 94.9 ± 7.5 μM].

To determine whether inhibition of the dehydrogenase activity of CtBP by hydroxyimine **9** and analogues **14a–m** is effective at inhibiting cancer cell growth, we carried out a short-term cell growth/viability assay (Table 1). HCT-116 $p53^{-/-}$ colorectal cancer cells were treated with the compounds for 72 h and cell growth and viability determined by MTT assay. The cellular IC_{50}'s for this set of compounds ranged from 0.23 to >10 mM. A complex structure–activity relationship was noted between in vitro enzyme inhibition and in vivo cell inhibitory activity, as demonstrated by the plot in Figure 3. A number of compounds appeared to have cytotoxic effects out of proportion to their in vitro activity, consistent with off-target or non-specific toxicity (**14c**, **14d**, **14f**, **14i**), while others had lower than expected cellular inhibitory effects consistent with instability or poor intracellular penetration (**14e**, **14k**). One subset of the compounds exhibited a relatively consistent correlation of in vitro and in vivo inhibitory activity (**14a**,**b**,**g**,**h**,**l**), with **14g** and **14h** demonstrating the strongest in vitro and in vivo inhibitory activity. However, the cellular IC_{50}'s for these compounds (0.85 to ~4 mM) were much higher than expected given their potent inhibition of recombinant CtBP2 (0.17–0.48 μM) in the in vitro enzyme inhibition assay.

One potential explanation for the poor correlation between the enzyme inhibition and cell inhibitory activity is that the hydroxyimine compounds are not stable to extended exposure to aqueous conditions and are hydrolyzed to the keto-acids. To evaluate the stability of the hydroxyimines, we incubated compounds **9**, **14g**, and **14h** in phosphate buffer (25 mM, pH 7.2) for 72 h and monitored for degradation by HPLC (see Fig. S1A–C in the Supplementary material). All three compounds were stable under these conditions for the entire 72 h and no hydrolysis products were observed.

Previous studies have shown that inhibition of CtBP de-represses the transcription of the pro-apoptotic gene Bik.[1] To determine whether the hydroxyimines that inhibit recombinant CtBP2 in vitro have a functional CtBP inhibition effect in a cellular environment, we performed an assay to measure restoration of Bik promoter transcription using a luciferase reporter system. In the absence of inhibitors, CtBP2 binds to the Bik promoter and prevents transcription of the firefly luciferase reporter gene cloned downstream of the Bik promoter. Functional inhibition of CtBP2 results in de-repression of the Bik promoter and an increase in the firefly luciferase signal. The hydroxyimine CtBP2 inhibitors **9**, **14g**, **14h**, **14f**, **14k**, and **1** were evaluated in this assay (Fig. 4). The hydroxyimines that were the best inhibitors of recombinant CtBP2 (**9**, **14g**, **14h**) also showed a strong increase in Bik transcription (**9**: 1.2-fold increase at 2 mM, 1.8-fold increase at 4 mM; **14g**: 1.32-fold increase at 1 mM, 2.91-fold increase at 2 mM; **14h**: 1.41-fold increase at 1 mM, 2.98-fold increase at 2 mM). For compounds **14g** and **14h**, the increase in Bik transcription could not be determined at 4 mM due to cellular cytotoxicity at this concentration. High concentrations of the substrate MTOB (**1**) resulted in little increase in Bik transcription in this assay (⩽1.15-fold increase at both 2 and 4 mM). Hydroxyimines **14f** (CtBP2 IC_{50} >100 μM; cellular IC_{50} = 1.24 mM) and **14k** (CtBP2 IC_{50} = 0.72 μM; cellular IC_{50} >10 mM) were also evaluated as control compounds and resulted in only modest increase in Bik transcription (**14f**: 1.45-fold increase at 2 mM; **14k**: 1.34-fold increase at 2 mM, 1.60-fold increase at 4 mM). The ~3-fold increase in Bik transcription by treatment with **14g** and **14h** (at 2 mM) demonstrates that the inhibition of cellular growth by these compounds most likely arises from on-target inhibition of CtBP and not off-target effects.[9]

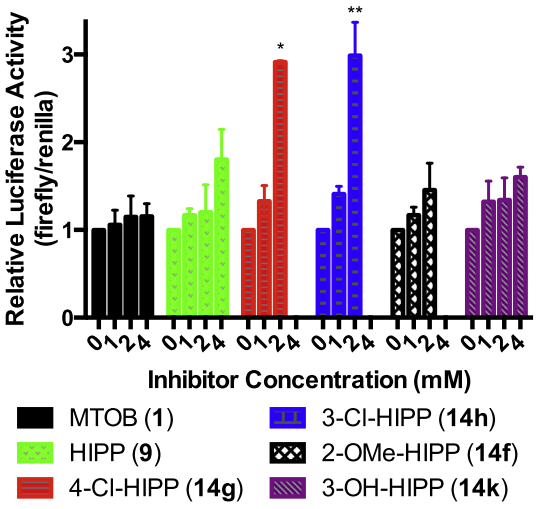

Figure 4. Change in Bik promoter expression in HCT-116 $p53^{-/-}$ cells upon treatment with CtBP inhibitors. $^{*}P$ <0.05 compared to **1**, **9**, **14f**, and **14h**. $^{**}P$ <0.05 compared to **1**, **9**, **14f**, and **14g**.

In parallel with this study to explore the structure–activity relationship of hydroxyimine **9**, our multidisciplinary team co-crystallized **9** with CtBP and NADH (Fig. 5). This crystal structure and associated biophysical data have been reported separately.[25] More detailed computational docking with this crystal structure model was performed to support the SAR studies. While no clear trend in docking scores versus protein or cellular inhibition IC_{50}'s was found, the docked poses of designed analogues at the CtBP active site revealed factors important for binding and inhibition (Fig. 6). Most importantly, the phenyl rings of the ligands fit well into a hydrophobic region primarily formed by Trp318, Tyr76 and Met327. Compounds **14a** and **14g** form stronger hydrophobic and aryl-X interactions in the pocket, compared to **14j**, where its polar (OH) substitution results in unfavorable hydrophobic-polar interactions. These results will inform our design of next-generation analogues.

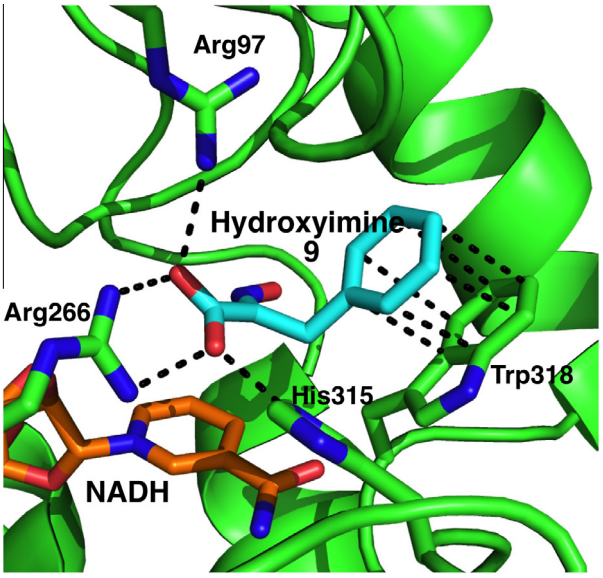

Figure 5. Crystal structure of CtBP1 with hydroxyimine **9** and NADH (PBDID: 4U6Q).

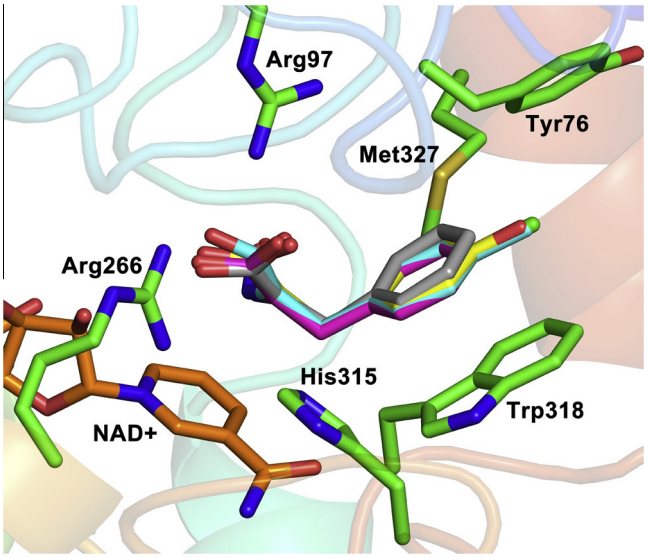

Figure 6. Docked poses of **9** (white), **14a** (cyan), **14g** (magenta) and **14j** (yellow) within CtBP active site.

2.3. Discussion

There is compelling evidence in the literature that targeting CtBP could be a highly tumor-selective and effective strategy for treating cancer. CtBP is activated as a transcriptional co-regulator only under conditions that are relatively unique to tumor cells (hypoxia and/or high NADH concentration). Disrupting the transcriptional co-regulatory function of CtBP in a tumorigenic environment has wide ranging effects on multiple cellular mechanisms, as was seen in the genomic study by Gardner and co-workers,[14] and can restore the natural, endogenous function of tumor suppressor genes.

While genetic inhibition of CtBP (with siRNA) and pharmacological inhibition with peptides are effective tools for studying the role of CtBP in cancer biology, small molecule inhibitors of CtBP are needed for further clinical drug development. Here we report the first small molecule inhibitors of CtBP dehydrogenase activity, and have optimized inhibition to a submicromolar level.

While **14g** and **14h** are effective inhibitors of recombinant CtBP dehydrogenase activity, high concentrations are still required to inhibit growth in cells and increase Bik promoter activity in the luciferase assay. Earlier work with the parent compound MTOB, however, suggests that in long term colony formation assays, GI_{50} values are usually 10-fold lower than those seen in short term assays, and these studies are ongoing with the hydroxyimine derivatives.

Even taking the possible 10-fold lower GI_{50} of CtBP inhibitors in long-term assays into account, the cellular inhibition for the current series of CtBP inhibitors remain 2–3 orders of magnitude higher than the in vitro IC_{50}'s. A possible rationale for this effect is that in cancer cells, CtBP has already formed transcriptional co-regulator complexes with NADH, transcription factors, and chromatin modifiers, and is not available for effective inhibitor binding. Binding of the inhibitor to CtBP either must break up the transcription complex or wait until the complex dissociates naturally in order to bind. This mechanistic model is consistent with our data that the compounds effectively bind to and inhibit the dimeric form of CtBP generated in the in vitro assay. Alternatively, the disparity between in vitro IC_{50} data and cell-based assays may be related to the incompletely understood relationship between enzymatic activity and transcriptional function of CtBP.

We are currently working to investigate this mechanistic model and develop analogues with improved activity in the cellular assays. We are also using these new CtBP inhibitors as tools for studying the role of CtBP in cell survival and migration, as well as the impact of restoring tumor suppressor gene expression and inhibiting oncogenes, such as *TIAM1*, in tumor cells. These ongoing investigations by our collaborative team will be reported in due course.

3. Conclusion

In conclusion, we have developed two compounds (**14g** and **14h**) that are substrate-competitive inhibitors of the dehydrogenase enzymatic activity of CtBP in vitro, inhibit growth in HCT-116 $p53^{-/-}$ colorectal cancer cells that express activated CtBP, and cause a ~3-fold increase in the transcription of the pro-apoptotic gene Bik in a luciferase reporter assay. These compounds serve as proof-of concept that substrate-competitive inhibition of CtBP dehydrogenase activity is a potential mechanism to reactivate tumor-suppressor gene expression.

4. Experimental section

4.1. Synthesis

4.1.1. General chemical methods

Reagents/chemicals, catalysts, solvents were purchased from Sigma-Aldrich, Fisher and Alfa-Aesar. The following compounds were purchased from commercial sources and tested for CtBP inhibition without further purification: 4-methylthio-2-oxobutyric acid (MTOB (**1**), Sigma-Aldrich), phenyl pyruvic acid (**3**, Sigma-Aldrich), 2-benzylacrylic acid (**5**, TCI America), benzylmalonic acid (**6**, Sigma Aldrich), anilino(oxo)acetic acid (**7**, Sigma-Aldrich), pyruvate (**10**, Sigma-Aldrich), hydrocinnamic acid (**11**, Sigma Aldrich), and phenylglyoxylic acid (**13**, Sigma-Aldrich). Analytical Thin Layer Chromatography (TLC) was performed using silica gel GHLF plates (Analtech Inc.). Flash chromatography was performed on Teledyne Isco CombiFlash® Rf instrument using RediSep Rf Normal-phase Flash Columns (4-gm, 12-gm, 24-gm or 40-gm). ^{1}H NMR and ^{13}C NMR experiments were recorded on Bruker 400 MHz NMR instrument in deuterated solvents—chloroform ($CDCl_3$), acetone (acetone-d_6), dimethyl sulfoxide (DMSO-d_6) or methanol (CD_3OD). All chemical shifts are reported in parts per million (ppm) with reference to chloroform, acetone, DMSO and methanol residual peaks at 7.26, 2.05, 2.50 and 3.31, respectively (^{1}H NMR spectra); 77.16, 29.84, 39.52 and 49.00, respectively (^{13}C NMR spectra). The data is reported as: chemical shifts (ppm), multiplicity (s = singlet, d = doublet, t = triplet, m = multiplet), coupling constant(s) (Hz) and integral values.

4.1.2. First generation and deconstruction analogues

3-Phenyl-2-thioxopropanoic acid (**4**): Rhodanine (1.25 g, 9.4 mmol), anhydrous sodium acetate (2.16 g, 26.4 mmol), and benzaldehyde (1.0 g, 9.4 mmol) were added to a vial followed by glacial acetic acid (17.8 mL, 0.53 M). The reaction was heated to 115 °C for three hours, upon which time the reaction had turned orange and developed a precipitate. The reaction mixture was cooled to room temperature and poured into ice water, which caused additional precipitate to form. Upon warming to room temperature, the precipitate was filtered and then dried in an oven for 36 h to afford a dry powder (1.66 g, 80% yield). This intermediate was dissolved in water (10 mL) and 6 N sodium hydroxide (10 mL) and heated to 95 °C for 1 h. The reaction mixture was cooled to room temperature, water (10 mL) was added, and 6 N HCl was added to crash out a white precipitate. This precipitate was filtered and purified by flash chromatography (silica gel, 5% MeOH/DCM) to afford the product (0.86 g, 63% yield). ^{1}H NMR (400 MHz, (DMSO-d_6) δ 7.74 (s, 1H), 7.68 (d, J = 7.4 Hz, 2H), 7.48 (t, 2H), 7.42-7.36 (m, 1H). HRMS $C_9H_7O_2S$ $[M-H]^-$ Expected: 179.0167, Found: 179.0164.

2-Hydrazono-3-phenylpropanoic acid (**8**): Phenylpyruvic acid (0.1 g, 0.61 mmol) was dissolved in ethanol (0.4 ml). Hydrazine (0.02 ml, 0.61 mmol) was added and the reaction mixture is stirred overnight at room temperature. Sodium carbonate (0.03 g, 0.31 mmol) was added and the reaction mixture was stirred for 2 h at room temperature. The precipitated solid was filtered and dried to give the title compound in 62% yield (0.07 g, 0.38 mmol). ^{1}H NMR (400 MHz, DMSO-d_6) δ 7.26 (d, J = 7.5 Hz, 2H), 7.19 (t, J = 7.7 Hz, 2H), 7.10 (t, J = 7.5 Hz, 1H), 6.26 (s, 2H), 3.78 (s, 2H); ^{13}C NMR (125 MHz, DMSO-d_6) δ 168.60, 146.52, 138.01, 128.68, 127.88, 125.37, 30.21. HRMS $C_9H_{10}N_2O_2$ $[M+Na]^-$ Expected: 201.0634, Found: 201.0622.

2-(Hydroxyimino)-3-phenylpropanoic acid (**9**): Phenyl pyruvic acid (3.0 g, 18.28 mmol) was dissolved in a solution of NaOH (2.2 g, 54.83 mmol) in water (1 ml). Hydroxylamine hydrochloride (1.9 g, 27.41 mmol) was added to the reaction and stirred overnight at room temperature. 1 N HCl was added to the reaction, the precipitated product was filtered and dried. The crude product was purified using flash chromatography (silica gel, 5% MeOH/DCM). Yield: 76% (2.50 g, 13.95 mmol). ^{1}H NMR (400 MHz, DMSO-d_6) δ 12.28 (s, 1H), 7.27 (m, 2H), 7.19 (m, 3H), 3.82 (s, 2H); ^{13}C NMR (125 MHz, DMSO-d_6) δ 165.14, 150.13, 136.68, 128.52, 128.32, 126.13, 29.85. HRMS $C_9H_9NO_3$ $[M-H]^-$ Expected: 178.0509, Found: 178.0494.

1-Phenylpropan-2-one (**12**): Phenylacetic acid (0.5 g, 3.7 mmol) was dissolved in DCM (9.2 ml). To this, *N*-(3-dimethylaminopropyl)-*N*′-ethylcarbodiimide hydrochloride (0.8 g, 4.4 mmol), 4-methylmorpholine (0.4 g, 3.7 mmol), *N*,*O*-dimethylhydroxylamine hydrochloride (0.4 g, 4.0 mmol) were added. The reaction mixture was stirred at room temperature for 4 h. It was concentrated and diethyl ether was added. The organic layer was washed with brine, dried over Na_2SO_4 and evaporated. Purification of the residue on silica gel (5:1 hexanes/EtOAc) afforded the product *N*-methoxy-*N*-methyl-2-phenylacetamide in 87% yield. 0.6 g (3.2 mmol) of this product was dissolved in ether (10.6 ml) under nitrogen at 0 °C. Methylmagnesium bromide solution (3.4 ml, 4.8 mmol, 1.4 M in THF/toluene 1:3) was added over 30 min. The reaction was stirred at 0 °C for 1 h and at room temperature for 30 min. It was quenched at 0 °C with the slow addition of 1 M HCl. The reaction was extracted with ether. The organic layer was washed with brine, dried over Na_2SO_4 and evaporated. Purification of the residue on silica gel (5:1 hexanes/EtOAc) afforded the product 1-phenylpropan-2-one in 89% yield (0.38 g, 2.83 mmol). ^{1}H NMR (400 MHz, MeOD) δ 7.21-7.33 (m, 5H), 3.75 (s, 2H), 2.15 (s, 3H); 13C NMR (125 MHz, MeOD) δ 209.24, 136.00, 130.58, 129.67, 127.97, 51.37, 29.27. HRMS $C_9H_{10}O$ $[M-H]^-$ Expected: 133.0659, Found: 132.0813.

4.1.3. Hydroxyimine analogues for structure–activity relationship study

4.1.3.1. Keto-acid intermediates. *General procedure* 1: Hydantoin (15.0 mmol) was dissolved in water (15.0 ml) at 70 °C. The solution was adjusted to pH 7 using saturated sodium bicarbonate solution. Ethanolamine (1.4 ml) was added and the temperature was raised to 90 °C. The corresponding aldehyde (15.0 mmol) in ethanol (15.0 ml) was added drop wise to the reaction mixture. The reaction was refluxed at 120 °C for 5–10 h. After being cooled to room temperature, the product was filtered, washed with alcohol/water (1:5) and dried to give the corresponding benzylhydantoin intermediate. This corresponding benzylhydantoin (8.98 mmol) was dissolved in 20% aqueous NaOH solution (28.4 ml) and refluxed at 100 °C for 3 h. After being cooled to room

temperature, 12 N HCl (11.8 ml) was added. Sodium bicarbonate was added to bring the pH to 7. The reaction mixture was extracted with ether until the ether layer was clear. This layer was discarded. To the aqueous layer, 12 N HCl (7.1 ml) was added. It was extracted with ether until no more acid was obtained. The ether layer was dried to give the crude keto-acid. It was recrystallized in water to give pure product, which was judged by proton NMR to exist as the enol tautomer.

2-Hydroxy-3-(p-tolyl)acrylic acid (**17a**): Procedure 1 was followed using 4-methylbenzaldehyde. Yield 54% (1.0 g, 5.61 mmol). ^{1}H NMR (400 MHz, MeOD) δ 7.64–7.66 (d, J = 8.1 Hz, 2H), 7.12–7.14 (d, J = 8.1 Hz, 2H), 6.46 (s, 1H), 2.32 (s, 3H); ^{13}C NMR (125 MHz, MeOD) δ 168.46, 141.49, 138.44, 133.49, 130.72, 129.87, 111.79, 21.28. HRMS $C_{10}H_{10}O_3$ $[M-H]^-$ Expected: 177.0557, Found: 177.0562.

2-Hydroxy-3-(m-tolyl)acrylic acid (**17b**): Procedure 1 was followed using 3-methylbenzaldehyde. Yield 57% (0.3 g, 1.68 mmol). ^{1}H NMR (400 MHz, MeOD) δ 7.57 (d, J = 4.1 Hz, 1H), 7.55 (s, 1H), 7.18–7.22 (t, J = 7.5 Hz, 1H), 7.03–7.05 (d, J = 7.9 Hz, 1H), 6.45 (s, 1H), 2.32 (s, 3H); ^{13}C NMR (125 MHz, MeOD) δ 170.0, 143.64, 140.38, 137.85, 132.89, 130.72, 129.55, 113.34, 23.07. HRMS $C_{10}H_{10}O_3$ $[M-H]^-$ Expected: 177.0557, Found: 177.0565.

2-Hydroxy-3-(4-methoxyphenyl)acrylic acid (**17d**): Procedure 1 was followed using 4-methoxybenzaldehyde. Yield 88% (1.8 g, 9.27 mmol). ^{1}H NMR (400 MHz, MeOD) δ 7.71–7.73 (d, J = 8.8 Hz, 2H), 6.88–6.90 (d, J = 8.9 Hz, 2H), 6.46 (s, 1H), 3.80 (s, 3H); ^{13}C NMR (125 MHz, MeOD) δ 168.61, 160.57, 140.55, 132.24, 129.08, 114.76, 111.83, 55.69. HRMS $C_{10}H_{10}O_4$ $[M-H]^-$ Expected: 193.0506, Found: 193.0511.

2-Hydroxy-3-(3-methoxyphenyl)acrylic acid (**17e**): Procedure 1 was followed using 3-methoxylbenzaldehyde. Yield 56% (0.5 g, 2.57 mmol). ^{1}H NMR (400 MHz, MeOD) δ 7.44 (t, J = 2 Hz, 1H), 7.20–7.29 (m, 2H), 6.79–6.82 (m, 1H), 6.46 (s, 1H), 3.79 (s, 3H); ^{13}C NMR (125 MHz, MeOD) δ 168.32, 161.04, 142.44, 137.66, 130.11, 123.52, 115.80, 114.39, 111.51, 55.62. HRMS $C_{10}H_{10}O_4$ $[M-H]^-$ Expected: 193.0506, Found: 193.0495.

2-Hydroxy-3-(2-methoxyphenyl)acrylic acid (**17f**): Procedure 1 was followed using 2-methoxybenzaldehyde. Yield 56% (0.23 g, 1.29 mmol). ^{1}H NMR (400 MHz, MeOD) δ 8.20–8.22 (m, 1H), 7.19–7.23 (m, 1H), 6.90–6.95 (m, 3H), 3.86 (s, 3H); ^{13}C NMR (125 MHz, MeOD) δ 168.64, 158.20, 141.79, 131.72, 129.78, 124.98, 121.41, 111.46, 105.03, 56.11. HRMS $C_{10}H_{10}O_4$ $[M-H]^-$ Expected: 193.0506, Found: 193.0496.

3-(4-Chlorophenyl)-2-hydroxyacrylic acid (**17g**): Procedure 1 was followed using 4-chlorobenzaldehyde. Yield 62% (1.1 g, 5.54 mmol). ^{1}H NMR (400 MHz, MeOD) δ 7.74–7.76 (d, J = 8.8 Hz, 2H), 7.30–7.32 (d, J = 8.5 Hz, 2H), 6.45 (s, 1H); ^{13}C NMR (125 MHz, MeOD) δ 168.05, 142.95, 135.22, 133.81, 132.06, 129.35, 110.01. HRMS $C_9H_7O_3Cl$ $[M-H]^-$ Expected: 197.0011, Found: 197.0016.

3-(2-Chlorophenyl)-2-hydroxyacrylic acid (**17i**): Procedure 1 was followed using 2-chlorobenzaldehyde. Yield 56% (0.3 g, 1.51 mmol). ^{1}H NMR (400 MHz, MeOD) δ 8.32–8.35 (d, J = 7.9 Hz, 1H), 7.38–7.40 (d, J = 8.1 Hz, 1H), 7.26–7.30 (t, J = 7.6 Hz, 1H), 7.19–7.21 (t, J = 7.8 Hz, 1H), 6.89 (s, 1H); ^{13}C NMR (125 MHz, MeOD) δ 167.97, 143.77, 134.42, 134.04, 132.20, 130.31, 129.41, 127.73, 105.93. HRMS $C_9H_7O_3Cl$ $[M-H]^-$ Expected: 197.0011, Found: 197.0010.

2-Hydroxy-3-(4-hydroxyphenyl)acrylic acid (**17j**): Procedure 1 was followed using 4-hydroxybenzaldehyde. Yield 74% (1.3 g, 7.22 mmol). ^{1}H NMR (400 MHz, MeOD) δ 7.62–7.64 (d, J = 8.6 Hz, 2H), 6.75–6.77 (d, J = 8.8 Hz, 2H), 6.45 (s, 1H); ^{13}C NMR (125 MHz, MeOD) δ 168.74, 158.19, 139.97, 132.41, 127.94, 116.15, 112.35. HRMS $C_9H_8O_4$ $[M-H]^-$ Expected: 179.0350, Found: 179.0354.

2-Hydroxy-3-(3-hydroxyphenyl)acrylic acid (**17k**): Procedure 1 was followed using 3-hydroxybenzaldehyde. Yield 88% (0.7 g, 3.89 mmol). ^{1}H NMR (400 MHz, (DMSO-d_6) δ 7.29 (s, 1H), 7.07–7.14 (m, 2H), 6.63–6.66 (m, 1H), 6.29 (s, 1H); ^{13}C NMR (125 MHz, (DMSO-d_6) δ 166.28, 157.11, 141.56, 135.96, 129.02, 120.48, 115.78, 114.47, 109.76. HRMS $C_9H_8O_4$ $[M-H]^-$ Expected: 179.0350, Found: 179.0348.

3-(4-Fluorophenyl)-2-hydroxyacrylic acid (**17l**): Procedure 1 was followed using 4-fluorobenzaldehyde. Yield 71% (0.5 g, 2.74 mmol). ^{1}H NMR (400 MHz, MeOD) δ 7.78–7.81 (m, 2H), 7.02–7.07 (t, J = 8.9 Hz, 2H), 6.47 (s, 1H); ^{13}C NMR (125 MHz, MeOD) δ 168.26, 164.52, 162.07, 142.02, 132.57, 132.65, 115.88, 116.10, 110.42. HRMS $C_9H_7O_3F$ $[M-H]^-$ Expected: 181.0306, Found: 181.0306.

3-(4-Cyanophenyl)-2-hydroxyacrylic acid (**17m**): Procedure 1 was followed using 4-cyanobenzaldehyde. Yield 70% (0.05 g, 0.26 mmol). ^{1}H NMR (400 MHz, (acetone-d_6) δ 8.62 (d, J = 1.7 Hz, 1H), 8.01 (d, J = 8.6 Hz, 2H), 7.76 (d, J = 8.6 Hz, 2H), 6.60 (s, 1H); ^{13}C NMR (125 MHz, (acetone-d_6) δ 167.49, 145.32, 141.54, 133.02, 132.69, 132.65, 131.03, 120.00, 110.87, 108.92. HRMS $C_{10}H_7NO_3$ $[M-H]^-$ Expected: 188.0353, Found: 188.0346.

General procedure 2: 1,4-Diacetylpiperazine-2,5-dione[27] (0.5 mmol) was dissolved in DMF (1 mL). Triethylamine (0.5 mmol) was added followed by corresponding aldehyde (0.5 mmol). The reaction mixture was stirred for 12 h at room temperature. It was extracted with DCM, washed with NH_4Cl solution. The organic layer was dried over Na_2SO_4 and evaporated. Purification of the residue on silica gel afforded the product (benzylidene)-piperazine-2,5-dione intermediate. This intermediate (0.1 mmol) was refluxed in 6 N HCl (4.0 ml) for 4 h. The reaction was cooled to room temperature, extracted with ether, dried over Na_2SO_4 and evaporated to give the crude keto-acid, which was recrystallized in water to give pure product and judged by proton NMR to exist as the enol tautomer.

2-Hydroxy-3-(o-tolyl)acrylic acid (**17c**): Procedure 2 was followed using 2-methylbenzaldehyde. Yield 58% (0.08 g, 0.45 mmol). ^{1}H NMR (400 MHz, (acetone-d_6) δ 8.18 (d, J = 8.2 Hz, 1H), 7.85 (s, 1H), 7.11-7.23 (m, 4H), 6.74 (s, 1H), 2.38 (s, 3H); ^{13}C NMR (125 MHz, (acetone-d_6) δ 167.10, 141.15, 137.11, 133.96, 130.84, 130.64, 128.34, 126.63, 107.60, 20.13. HRMS $C_{10}H_{10}O_3$ $[M-H]^-$ Expected: 177.0557, Found: 177.0549.

3-(3-Chlorophenyl)-2-hydroxyacrylic acid (**17h**): Procedure 2 was followed using 3-chlorobenzaldehyde. Yield 56% (0.12 g, 0.60 mmol). ^{1}H NMR (400 MHz, (acetone-d_6) δ 7.96 (t, J = 1.96 Hz, 1H), 7.76 (dt, J = 7.8 Hz, 1H), 7.25–7.41 (m, 3H), 6.54 (s, 1H), 4.28 (s, 0.6H), 4.05 (d, J = 6.2 Hz, 0.5H); ^{13}C NMR (125 MHz, (acetone-d_6) δ 166.54, 137.85, 134.59, 130.74, 130.67, 129.80, 128.83, 127.99, 109.31. HRMS $C_9H_7O_3Cl$ $[M-H]^-$ Expected: 197.0011, Found: 197.0005.

4.1.3.2. Hydroxyimine analogues. *General procedure* 3: The corresponding keto-acid (0.50 mmol) was dissolved in a solution of NaOH (1.51 mmol) in water (1 ml). Hydroxylamine hydrochloride (0.76 mmol) was added to the reaction and stirred overnight at room temperature. 1 N HCl was added to the reaction, the precipitated product was filtered and dried. The crude product was purified using flash chromatography (silica gel, 5% MeOH/DCM) as necessary.

2-(Hydroxyimino)-3-p-tolylpropanoic acid (**14a**): Title compound was prepared following general procedure 3. Yield 55% (0.03 g, 0.16 mmol). ^{1}H NMR (400 MHz, MeOD) δ 7.05–7.14 (m, 4H), 3.86 (s, 2H), 2.27 (s, 3H); ^{13}C NMR (125 MHz, MeOD) δ 166.90, 152.35, 136.96, 134.84, 129.96, 129.89, 30.51, 21.03. HRMS $C_{10}H_{11}NO_3$ $[M-H]^-$ Expected: 192.0666, Found: 192.0673.

2-(Hydroxyimino)-3-m-tolylpropanoic acid (**14b**): Title compound was prepared following general procedure 3. Yield 74% (0.04 g, 0.21 mmol). ^{1}H NMR (400 MHz, MeOD) δ 7.03–7.13 (m, 3H), 6.98 (d, J = 7.31 Hz, 1H), 3.87 (s, 2H), 2.28 (s, 3H); ^{13}C NMR

(125 MHz, MeOD) δ 166.88, 152.22, 139.03, 137.84, 130.61, 129.26, 128.02, 127.02, 30.85, 21.42. HRMS $C_{10}H_{11}NO_3$ $[M-H]^-$ Expected: 192.0666, Found: 192.0656.

2-(Hydroxyimino)-3-o-tolylpropanoic acid (**14c**): Title compound was prepared following general procedure 3. Yield 92% (0.12 g, 0.62 mmol). ^{1}H NMR (400 MHz, (acetone-d_6) δ 7.01-7.10 (m, 4H), 3.88 (s, 2H), 2.35 (s, 3H); ^{13}C NMR (125 MHz, (acetone-d_6) δ 167.77, 153.63, 137.10, 136.37, 130.67, 129.10, 126.82, 126.60, 28.37, 19.93. HRMS $C_{10}H_{11}NO_3$ $[M-H]^-$ Expected: 192.0666, Found: 192.0652.

2-(Hydroxyimino)-3-(4-methoxyphenyl)propanoic acid (**14d**): Title compound was prepared following general procedure 3. Yield 71% (0.08 g, 0.36 mmol). ^{1}H NMR (400 MHz, MeOD) δ 7.18 (d, J = 8.6 Hz, 2H), 6.79 (d, J = 8.8 Hz, 2H), 3.86 (s, 2H), 3.74 (s, 3H); ^{13}C NMR (125 MHz, MeOD) δ 167.48, 159.71, 153.20, 131.07, 130.09, 114.79, 55.67, 30.16. HRMS $C_{10}H_{11}NO_4$ $[M-H]^-$ Expected: 208.0615, Found: 208.0601.

2-(Hydroxyimino)-3-(3-methoxyphenyl)propanoic acid (**14e**): Title compound was prepared following general procedure 3. Yield 72% (0.08 g, 0.37 mmol). ^{1}H NMR (400 MHz, MeOD) δ 7.13–7.17 (t, J = 8.1 Hz, 1H), 6.83 (m, 2H), 6.74 (dd, J = 8.3 Hz, 1H), 3.89 (s, 2H), 3.75 (s, 3H); ^{13}C NMR (125 MHz, MeOD) δ 166.87, 161.21, 152.07, 139.41, 130.29, 122.35, 115.73, 112.86, 55.56, 30.95. HRMS $C_{10}H_{11}NO_4$ $[M-H]^-$ Expected: 208.0615, Found: 208.0612.

2-(Hydroxyimino)-3-(2-methoxyphenyl)propanoic acid (**14f**): Title compound was prepared following general procedure 3. Yield 56% (0.07 g, 0.33 mmol). ^{1}H NMR (400 MHz, (acetone-d_6) δ 7.17 (t, J = 7.8 Hz, 1H), 7.00 (d, J = 7.6 Hz, 1H), 6.93 (d, J = 8.5 Hz, 1H), 6.83 (t, J = 7.6 Hz, 1H), 3.90 (s, 2H), 3.82 (s, 3H); ^{13}C NMR (125 MHz, (acetone-d_6) δ 165.17, 158.28, 151.76, 129.60, 28.34, 125.57, 121.06, 111.32, 55.72, 25.53. HRMS $C_{10}H_{11}NO_4$ $[M-H]^-$ Expected: 208.0615, Found: 208.0607.

3-(4-Chlorophenyl)-2-(hydroxyimino)propanoic acid (**14g**): Title compound was prepared following general procedure 3. Yield 56% (0.06 g, 0.28 mmol). ^{1}H NMR (400 MHz, DMSO-d_6) δ 12.34 (br s, 1H), 7.33 (d, J = 8.5 Hz, 2H), 7.20 (d, J = 8.5 Hz, 2H), 3.79 (s, 2 H); ^{13}C NMR (125 MHz, MeOD) δ 166.71, 151.68, 136.88, 133.20, 131.63, 129.40, 30. 39. HRMS $C_9H_8NO_3Cl$ $[M-H]^-$ Expected: 212.0120, Found: 212.0102.

3-(3-Chlorophenyl)-2-(hydroxyimino)propanoic acid (**14h**): Title compound was prepared following general procedure 3. Yield 66% (0.15 g, 0.70 mmol). ^{1}H NMR (400 MHz, DMSO-d_6) δ 7.24–7.34 (m, J = 8.8 Hz, 3H), 7.17 (d, J = 7.3 Hz, 1H), 3.82 (s, 2H); ^{13}C NMR (125 MHz, DMSO-d_6) δ 165.16, 139.26, 132.81, 130.14, 128.32, 127.32, 126.14, 29.64. HRMS $C_9H_8O_3NCl$ $[M-H]^-$ Expected: 212.0120, Found: 212.0108.

3-(2-Chlorophenyl)-2-(hydroxyimino)propanoic acid (**14i**): Title compound was prepared following general procedure 3. Yield 54% (0.02 g, 0.07 mmol). ^{1}H NMR (400 MHz, DMSO-d_6) δ 7.41–7.44 (m, 1H), 7.21–7.28 (m, 2H), 7.03 (m, 1H), 3.88 (s, 2H); ^{13}C NMR (125 MHz, DMSO-d_6) δ 164.97, 149.01, 134.08, 132.83, 129.22, 129.11, 127.96, 127.11, 27.93. HRMS $C_9H_8O_3NCl$ $[M-H]^-$ Expected: 212.0120, Found: 212.0134.

2-(Hydroxyimino)-3-(4-hydroxyphenyl)propanoic acid (**14j**): Title compound was prepared following general procedure 3. Yield 91% (0.10 g, 0.51 mmol). ^{1}H NMR (400 MHz, MeOD) δ 7.08 (d, J = 8.5 Hz, 2H), 6.66 (d, J = 8.5 Hz, 2H), 3.80 (s, 2H); ^{13}C NMR (125 MHz, MeOD) δ 166.93, 156.93, 152.63, 131.06, 128.70, 116.13, 30.03. HRMS $C_9H_9NO_4$ $[M-H]^-$ Expected: 194.0459, Found: 194.0459.

2-(Hydroxyimino)-3-(3-hydroxyphenyl)propanoic acid (**14k**): Title compound was prepared following general procedure 3. Yield 65% (0.07 g, 0.36 mmol). ^{1}H NMR (400 MHz, DMSO-d_6) δ 7.04 (t, J = 8.0 Hz, 1H), 6.55–6.62 (m, 3H), 3.72 (s, 2H); ^{13}C NMR (125 MHz, DMSO-d_6) δ 165.18, 157.22, 137.89, 129.09, 119.24, 115.44, 113.07, 48.52, 29.74. HRMS $C_9H_9NO_4$ $[M-H]^-$ Expected: 194.0459, Found: 194.0442.

3-(4-Fluorophenyl)-2-(hydroxyimino)propanoic acid (**14l**): Title compound was prepared following general procedure 3. Yield 74% (0.08 g, 0.41 mmol). ^{1}H NMR (400 MHz, DMSO-d_6) δ 7.20–7.24 (m, 2H), 7.10 (t, J = 8.8 Hz, 2H), 3.79 (s, 2H); ^{13}C NMR (125 MHz, MeOD) δ 165.06, 161.94, 159.54, 150.03, 132.82, 132.79, 130.38, 130.30, 115.12, 114.91, 29.06. HRMS $C_9H_8NO_3F$ $[M-H]^-$ Expected: 196.0415, Found: 196.0398.

3-(4-Cyanophenyl)-2-(hydroxyimino)propanoic acid (**14m**): Title compound was prepared following general procedure 3. Yield 64% (0.09 g, 0.44 mol). ^{1}H NMR (400 MHz, DMSO-d_6) δ 7.74 (d, J = 7.6 Hz, 2H), 7.37 (d, J = 8.1 Hz, 2H), 3.89 (s, 2H); ^{13}C NMR (125 MHz, DMSO-d_6) δ 164.93, 149.11, 142.74, 132.26, 129.52, 118.77, 109.06, 30.20. HRMS $C_{10}H_8N_2O_3$ $[M-H]^-$ Expected: 203.0462, Found: 203.0452.

4.2. Biological assays

4.2.1. Protein production and purification of CtBP2

Truncated CtBP2 (amino acids 31-384), which lacks both the N- and C-terminal domains, was expressed as a His_6-tagged protein in BL21-CodonPlus®(DE3)-RIL competent cells (Stratagene). Protein expression was induced in cultures with 200 μM IPTG for 4 h and cells were homogenized and incubated in the presence of NiNTA beads (Thermo Scientific). CtBP2(31-384) was eluted with 300 mM imidazole after several washes and further purified by overnight dialysis and passage through a 6–8000 kDa MWCO filter (Fisher Scientific). Purity was assessed by Coomassie stain (Invitrogen).

4.2.2. Inhibition of dehydrogenase activity of recombinant CtBP (NADH inhibition assay)[22]

Purified CtBP2 in 50% glycerol was added to 150 μM NADH, 48 μM MTOB and various concentrations of inhibitor in buffer containing 25 mM HEPES, pH 7.1, 25 mM potassium chloride, and 1 mM DTT. The final concentration of CtBP2 was 40 μg/mL (986 nM) per reaction. Inhibitors dissolved in DMSO constituted 1% of the total volume. For compounds **4**–**13**, inhibitor concentrations ranging from 300 μM to 10 μM and a no-drug (DMSO) control were tested. For **9** and analogues **14a**–**m**, inhibitor concentrations of 5 μM, 2.5 μM, 1 μM, 500 nM, 100 nM, 50 nM, 10 nM, and 0 nM (DMSO control) were used. Three triplicate runs were performed for each inhibitor.

Reaction components were added to 96-well UV-Star Microplates (Greiner Bio-One) and upon addition of CtBP, reactions were mixed vigorously and immediately read by a Synergy H1 microplate reader (BioTek). Absorbance was recorded at A = 340 nm every 30 s for 15 min at 25 °C to measure CtBP2 dehydrogenase function (NADH, but not NAD+ absorbs light at 340 nm). Change in absorbance was plotted after 15 min and IC_{50} concentrations were determined using Prism (Graphpad, Version 5.04).

4.2.3. Inhibition of dehydrogenase activity of lactate dehydrogenase (LDH)

Lactate dehydrogenase (Sigma-Aldrich L1254, 0.5 U/mL, in 50% glycerol) was added to 300 μM NADH, 200 μM sodium pyruvate, and various concentrations of inhibitor in 100 mM phosphate buffer (pH 7.2). Inhibitors dissolved in DMSO constituted 1.25% of the total reaction volume (80 μL). Inhibitor concentrations of 192, 96, 48, 24, 12, 6, and 3 μM and 0 μM (DMSO control) were used. Three triplicate runs were performed for each inhibitor. Sodium oxamate was used as a control for LDH inhibition and was found to have an IC_{50} of 45.8 ± 1.9 μM.

Reaction components were added to 96-well Microplates (Greiner Bio-One), mixed, and immediately read on a FlexStation 3 microplate reader (Molecular Devices). Absorbance was recorded at A = 340 nm every 10 s for 30 min at 28 °C to measure LDH dehydrogenase function (NADH, but not NAD^+ absorbs light at 340 nm).

Change in absorbance was plotted and IC_{50} concentrations were determined using Prism (Graphpad).

4.2.4. Inhibition of cell growth (MTT assay)

HCT-116 $p53^{-/-}$ colorectal cancer cell (~1000 cells) in 100 μL media were plated in a 96 well plate. After a 24-hour incubation, inhibitors in DMSO were further diluted in $NaHCO_3$ (0.8% diluted DMSO final volume/well) and added to plates at 4, 2, 1, and 0.5 mM concentrations. 72 h after addition of inhibitor, 20 μL of MTT solution (Alfa Aesar) was added to each well and cells were incubated a further 4 h. Media was then aspirated and the MTT metabolic product formazan was resuspended in 200 μL DMSO. Optical density was measured at 560 nm (subtracting background at 670 nm) using a microplate reader and IC_{50} concentrations were determined using Prism (Graphpad, Version 5.04).

4.2.5. Restoration of Bik transcription (Luciferase assay)

HCT-116 $p53^{-/-}$ colorectal cancer cell (800 cells per well) were plated in a 96-well plate. After 24 h, cells were transfected with pCDNA3-V5-CtBP2, the transcription factor pCDNA3-V5-KLF8, the firefly luciferase vector pGL3-Bik (promoter region −1710 to +203), and control luciferase plasmid expressing Renilla luciferase, pRL-TK, using Lipofectamine 2000 (Thermo Fisher). Following a further 24-h incubation, vehicle (DMSO) or inhibitors (**9**, **14g**, **14h**, **14f**, **14k**, and **1**) were added to their final concentrations (1, 2, or 4 mM) and the expression of luciferase reporter genes was determined using the Dual Luciferase assay (Promega). For analysis, Firefly expression was normalized to Renilla control, and values were reported as a proportion of the luciferase expression of the vehicle (DMSO) control. Statistical analyses were determined by One-way ANOVA using a Tukey's post-test using Graphpad Prism software for 2 mM drug concentrations. Data points display the average of three independent experiments, and error bars represent standard deviation.

4.3. Stability of hydroxyimines to aqueous hydrolysis

Compounds **9**, **14g**, and **14h** were diluted in 25 mM phosphate buffer (pH 7.2) to a final concentration of 4 mM. Compounds were incubated for the time indicated and then analyzed by HPLC (Agilent 1200). Aliquots (20 μL) were injected on a C18 column at a flow rate of 1.0 mL/min and eluted over 12 min (Linear Gradient: 95% H_2O/5% ACN to 5% H_2O/95% ACN). Compound elution was detected at 254 nm on a diode-array detector. The appropriate keto-acid (**3**, **17g**, or **17h**) were used as controls to monitor for hydrolysis of the oxime to the keto-acid.

4.4. HINT scoring

Analogues of hydroxyimine **9** were modeled with SYBYL-X 2.1 (Tripos Inc.); Gasteiger–Hückel charges were assigned and models were energy minimized with the Tripos forcefield (10,000 iterations, termination gradient of 0.01 kcal/mol-Å). The crystal structure[25] of CtBP1/**9**/NAD^+ was used as the target for docking studies using GOLD v5.2,[28] with the binding defined as all the residues within 10 Å of the bound ligand **9**. Since the ligands are analogs of **9**, it is reasonable to expect that they will adopt binding modes very similar to that of the parent compound. Thus, the binding pose of **9** defined a scaffold match constraint, i.e., the common substructure forced the corresponding atoms of ligands to lie in the exact, or very close, position within the binding site. Default GOLD genetic algorithm parameters were used and a total of 50 solutions per compound were generated. The generated conformations were re-ranked using the free-energy based HINT force-field,[29] that quantifies all non-bonded interactions in a biological environment, including hydrogen-bonding, electrostatic interactions, hydrophobic interactions as well as desolvation energy. The ligand in its most energetically favorable binding conformation and the CtBP1/NAD^+ complex were subjected to minimization (Powell, 2500 iterations, termination gradient 0.01 kcal/mol-Å), to remove steric clashes and optimize the protein-ligand interactions within the active site. HINT scores for the thus optimized complex were then recalculated.

Acknowledgments

The authors thank Professor Richard G. Moran and the Massey Cancer Center Developmental Therapeutics group for valuable feedback and suggestions. This research was supported by a Pilot Project Grant from the VCU Massey Cancer Center (to K.C.E. and S.R.G.) and VCU Massey Cancer Center Shared Resource Cores supported in part with funding from NIH-NCI Cancer Center Support Grant P30 CA016059.

Supplementary data

Supplementary data (Table S1, Figure S2A–C, and NMR spectra for compounds) associated with this article can be found, in the online version, at http://dx.doi.org/10.1016/j.bmc.2016.04.037.

References and notes

1. Straza, M. W.; Paliwal, S.; Kovi, R. C.; Rajeshkumar, B.; Trenh, P.; Parker, D.; Whalen, G. F.; Lyle, S.; Schiffer, C. A.; Grossman, S. R. *Cell Cycle* **2010**, *9*, 3764.
2. Deng, Y.; Deng, H.; Liu, J.; Han, G.; Malkoski, S.; Liu, B.; Zhao, R.; Wang, X.-J.; Zhang, Q. *Mol. Carcinog.* **2012**, *51*, 500.
3. Barroilhet, L.; Yang, J.; Hasselblatt, K.; Paranal, R. M.; Ng, S. K.; Rauh-Hain, J. A.; Welch, W. R.; Bradner, J. E.; Berkowitz, R. S.; Ng, S. W. *Oncogene* **2013**, *32*, 3896.
4. Subramanian, T.; Chinnadurai, G. *FEBS Lett.* **2003**, *540*, 255.
5. Shi, Y.; Sawada, J.-I.; Sui, G.; Affar, E. B.; Whetstine, J. R.; Lan, F.; Ogawa, H.; Po-Shan Luke, M.; Nakatani, Y.; Shi, Y. *Nature* **2003**, *422*, 735.
6. Chinnadurai, G. *Int. J. Biochem. Cell Biol.* **2007**, *39*, 1593.
7. Grooteclaes, M.; Deveraux, Q.; Hildebrand, J.; Zhang, Q.; Goodman, R. H.; Frisch, S. M. *Proc. Natl. Acad. Sci. U.S.A.* **2003**, *100*, 4568.
8. Paliwal, S.; Kovi, R. C.; Nath, B.; Chen, Y.-W.; Lewis, B. C.; Grossman, S. R. *Cancer Res.* **2007**, *67*, 9322.
9. Kovi, R. C.; Paliwal, S.; Pande, S.; Grossman, S. R. *Cell Death Differ.* **2010**, *17*, 513.
10. Zhang, Q.; Wang, S.-Y.; Nottke, A. C.; Rocheleau, J. V.; Piston, D. W.; Goodman, R. H. *Proc. Natl. Acad. Sci. U.S.A.* **2006**, *103*, 9029.
11. Chen, Y.-W.; Paliwal, S.; Draheim, K.; Grossman, S. R.; Lewis, B. C. *Cancer Res.* **2008**, *68*, 476.
12. Paliwal, S.; Pande, S.; Kovi, R. C.; Sharpless, N. E.; Bardeesy, N.; Grossman, S. R. *Mol. Cell. Biol.* **2006**, *26*, 2360.
13. Jin, W.; Scotto, K. W.; Hait, W. N.; Yang, J.-M. *Biochem. Pharmacol.* **2007**, *74*, 851.
14. Di, L.-J.; Byun, J. S.; Wong, M. M.; Wakano, C.; Taylor, T.; Bilke, S.; Baek, S.; Hunter, K.; Yang, H.; Lee, M.; Zvosec, C.; Khramtsova, G.; Cheng, F.; Perou, C. M.; Ryan Miller, C.; Raab, R.; Olopade, O. I.; Gardner, K. *Nat. Commun.* **2013**, *4*, 1449.
15. Fjeld, C. C.; Birdsong, W. T.; Goodman, R. H. *Proc. Natl. Acad. Sci. U.S.A.* **2003**, *100*, 9202.
16. Mani-Telang, P.; Sutrias-Grau, M.; Williams, G.; Arnosti, D. N. *FEBS Lett.* **2007**, *581*, 5241.
17. Zhang, Q.; Piston, D. W. *Science* **2002**, *295*, 1895.
18. Kumar, V.; Carlson, J. E.; Ohgi, K. A.; Edwards, T. A.; Rose, D. W.; Escalante, C. R.; Rosenfeld, M. G.; Aggarwal, A. K. *Mol. Cell* **2002**, *10*, 857.
19. Thio, S. S. C.; Bonventre, J. V.; Hsu, S. I.-H. *Nucleic Acids Res.* **2004**, *32*, 1836.
20. Birts, C. N.; Nijjar, S. K.; Mardle, C. A.; Hoakwie, F.; Duriez, P. J.; Blaydes, J. P.; Tavassoli, A. *Chem. Sci.* **2013**, *4*, 3046.
21. Blevins, M. A.; Kouznetsova, J.; Krueger, A. B.; King, R.; Griner, L. M.; Hu, X.; Southall, N.; Marugan, J. J.; Zhang, Q.; Ferrer, M.; Zhao, R. *J. Biomol. Screen.* **2015**, *20*, 663.
22. Achouri, Y.; Noël, G.; Van Schaftingen, E. *Biochem. Biophys. Res. Commun.* **2007**, *352*, 903.
23. May, T.; Yang, J.; Shoni, M.; Liu, S.; He, H.; Gali, R.; Ng, S.-K.; Crum, C.; Berkowitz, R. S.; Ng, S.-W. *Neoplasia* **2013**, *15*, 600.
24. Hilbert, B. J.; Grossman, S. R.; Schiffer, C. A.; Royer, W. E., Jr. *FEBS Lett.* **2014**, *588*, 1743.
25. Hilbert, B. J.; Morris, B. L.; Ellis, K. C.; Paulsen, J. L.; Schiffer, C. A.; Grossman, S. R.; Royer, W. E. *ACS Chem. Biol.* **2015**, *10*, 1118.
26. Sarkar, A.; Kellogg, G. E. *Curr. Top. Med. Chem.* **2010**, *10*, 67.
27. Balducci, D.; Conway, P. A.; Sapuppo, G.; Müller-Bunz, H.; Paradisi, F. *Tetrahedron* **2012**, *68*, 7374.
28. Verdonk, M. L.; Cole, J. C.; Hartshorn, M. J.; Murray, C. W.; Taylor, R. D. *Proteins: Struct. Funct. Bioinf.* **2003**, *52*, 609.
29. Kellogg, G. E.; Abraham, D. J. *Eur. J. Med. Chem.* **2000**, *35*, 651.